Quantitative Mass Spectrometry Independence from Matrix Effects and Detector Saturation Achieved by Flow Injection Analysis with Real-Time Infinite Dilution

- Supporting Information -

Sergio C. Nanita

DuPont Crop Protection, Stine-Haskell Research Center, 1090 Elkton Road, Newark, Delaware 19714, U.S.A.

Phone: 1-302-451-0031

Email: sergio.c.nanita@dupont.com

TABLE OF CONTENTS

1.0 Experimental Section (Additional Information)

1.1 Reagents and reference standards

Acetonitrile and water were purchased from EMD Science (Gibbstown, New Jersey, USA) as HPLC-grade solvents. Ammonium formate, which was used as salting out extraction agent, was obtained from Sigma-Aldrich (Saint Louis, Missouri, USA). The reference substances of bioactive molecules used in this study were the pesticides hexazinone, triflusulfuron methyl, flupyrsulfuron methyl and chlorantraniliprole. These materials were synthesized by DuPont Crop Protection, Global Technology Division, E. I. du Pont de Nemours and Company, and certified to be of analytical standard grade (>98% pure). The chemical structures of the analytes tested appear in Table S-1.

Table S-1. *Chemical structures and description of the representative analytes tested.*

Name, structure, formula, nominal mass (Da)	Description
Chlorantraniliprole 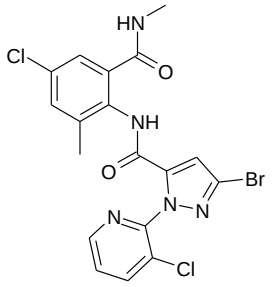 Nominal Mass (in Daltons) =481 Molecular Formula =C18H14BrCl2N5O2	- Anthranilic diamide insecticide - Ryanodine receptor activator
Flupyrsulfuron methyl 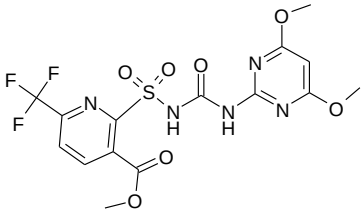 Nominal Mass (in Daltons) =465 Molecular Formula =C15H14F3N5O7S	- Sulfonylurea herbicide - Acetolactate Synthase (ALS) inhibitor
Hexazinone 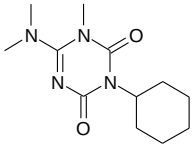 Nominal Mass (in Daltons) =252 Molecular Formula =C12H20N4O2	- Triazinone herbicide - Photosynthesis inhibitor

Name, structure, formula, nominal mass (Da)	Description
Triflusulfuron methyl 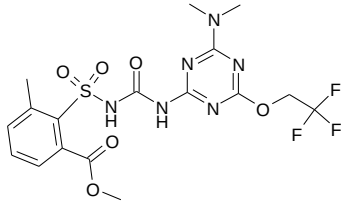 Nominal Mass (in Daltons) =492 Molecular Formula =C17H19F3N6O6S	- Sulfonylurea herbicide - Acetolactate Synthase (ALS) inhibitor

1.2 Control samples of complex matrices

Control samples of rat urine, rat blood, wheat grain, strawberry, canola seed and corn meal were available from previous DuPont studies. Samples of strawberry from a field in California that was treated with chlorantraniliprole were available together with analytical data generated using well-established techniques, particularly high-performance liquid chromatography MS/MS and FIA/MS/MS with matrix-matched standards.[22] Re-analysis of those samples by the proposed method was conducted to compare the new technique to the other two methods. The samples of raw and processed agricultural commodities were homogenized with dry ice and a Hobart processor. The dry ice was allowed to sublime. All samples were stored under freezer conditions when not in use. They were allowed to thaw prior to each use.

1.3 Preparation of salting out agent for sample extraction

A concentrated 34% w/w aqueous solution of ammonium formate was prepared and used as salting out agent during sample extraction. A total of 88 g of ammonium formate were weighed into a 250-mL bottle. A total of 170.0 g of water were added. The bottle was capped and shaken until all solid dissolved. The volume of this solution was ~230 mL and it was not adjusted further. Multiple batches of this solution were prepared for extraction of samples that were analyzed using two different API-5000 triple quadrupole mass spectrometers.

1.4 Preparation of carrier solvent for flow injection analysis

The carrier liquid used in flow injection mass spectrometric analysis was prepared to simulate the reagent blank composition. This ensures that real-time sample dilution achieved with the flow injection system maintains a relatively constant background solvent composition. Approximately 351 g of acetonitrile were weighed into a 500-mL glass bottle. This was calculated to be 450 mL (acetonitrile density = 0.78 g/mL). Then, 50 mL of pooled/undiluted acetonitrile-rich (top) layers from reagent blank extracts were added to the bottle. Note that this 10-fold dilution matches that of the samples (see experimental section, main manuscript). The bottle was capped and shaken. Two batches of carrier liquid were prepared; one for each API-5000 mass spectrometer used. The volume of carrier liquid prepared on each batch is estimated to be sufficient to analyze >3000 sample injections.

Table S-2. *Tandem mass spectrometry conditions used for FIA/MS/MS analysis.*

Analyte	Precursor ion	Q1 Parent Ion (m/z)	Q3 Fragment Ion (m/z)	EP	DP (V)	CE (V)	CXP	Dwell time (ms)
Chlorantraniliprole	$[M+H]^+$	484	453	12	110	26	25	5
Flupyrsulfuron methyl	$[M+H]^+$	466	182	10	75	40	25	5
Hexazinone	$[M+H]^+$	253	171	10	116	23	26	5
Triflusulfuron methyl	$[M+H]^+$	493	264	10	75	40	25	5

Abbreviations: Q1 = quadrupole 1; Q3 = quadrupole 3; EP = entrance potential; CE = collision energy; DP = declustering potential; collision cell exit potential.

1.5 Synchronization of FIA/MS/MS chronograms of samples and standards

Some sample chronograms needed to be synchronized with the reference standards chronograms. This was done by simply shifting the sample data points along the time axis, as shown in Figures S-1 and S-2, such that the intensity maxima of both data sets were aligned. The example presented (Figures S-1 and S-2) is for the quantitation of hexazinone in strawberry extract; the average reference standard ion chronogram obtained during system calibration is shown for comparison. Note that small errors in synchronization between the reference standard and sample data sets resulted in relatively large errors in the calculated A_m vs. S_{norm} function. Interestingly, the measurement method provided a reliable qualitative indication of data synchronization. Under synchronized conditions, $A_m(S_{norm})$ data points obtained from the peak front and peak tail should overlap; whereas unsynchronized data sets should yield two discrete $A_m(S_{norm})$ functions. An example of this phenomenon appears in Figure S-1c and S-1d. Consequently, some data sets required to be synchronized (aligned) with respect to the calibration standard data set. This was done by simply shifting the sample data points along the time axis, as shown in Figure S-2, such that the intensity maxima of both data sets were aligned (Figure S-2a) and the resulting A_m vs. S_{norm} data obtained were aligned (Figure S-2c and S-2d).

Unsynchronized average FIA/MS/MS ion chronograms of hexazinone in a reference standard and strawberry sample, and the resulting A_m vs. S_{norm} function

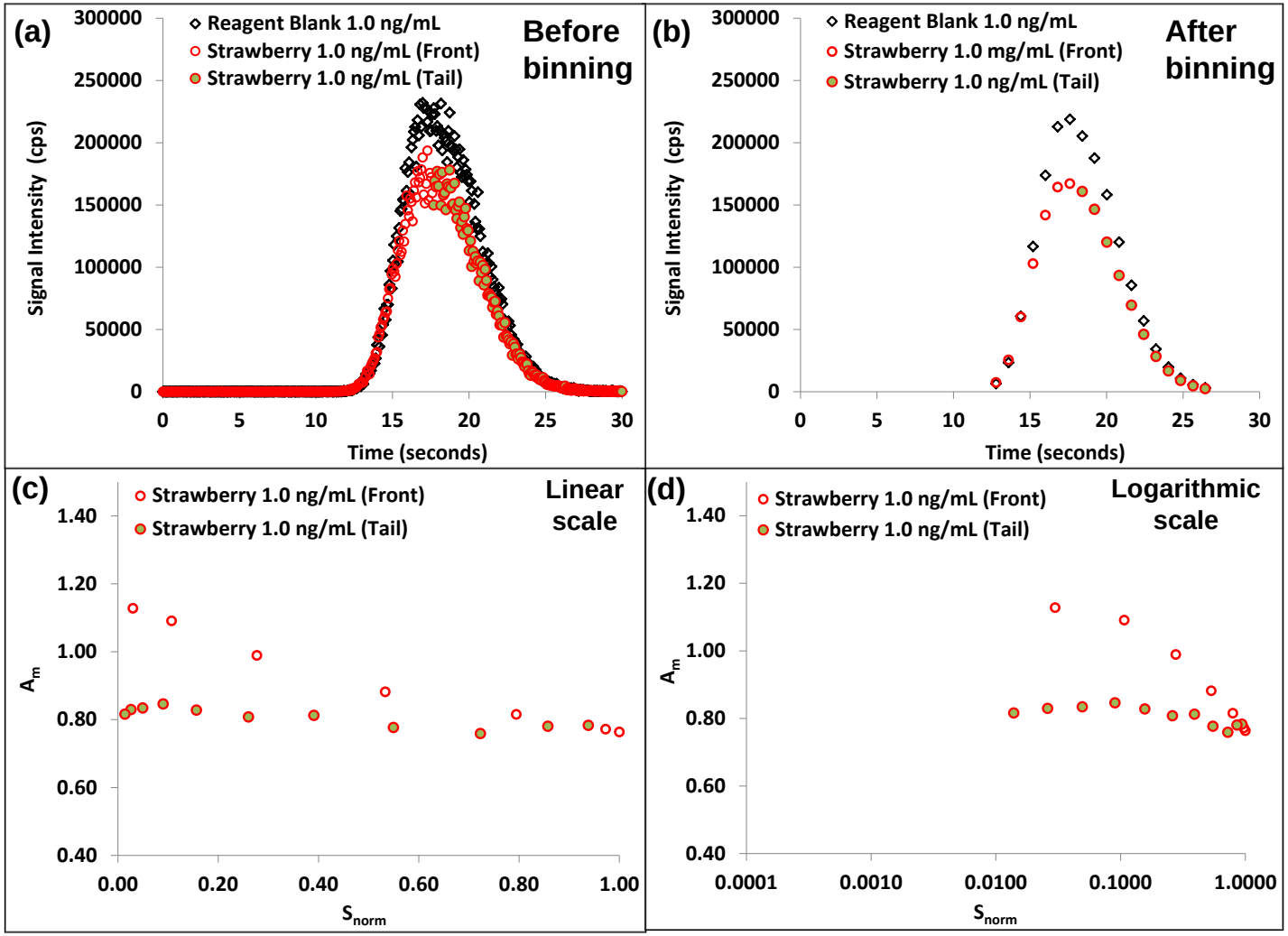

Figure S-1. *Calculation of A_m as a function of S_{norm} for hexazinone in strawberry extract from* ***unsynchronized*** *data. Averaged MS/MS chronograms: (a) all data points and (b) binned. The resulting A_m vs. S_{norm} graphs are shown in (c) linear and (d) logarithmic abscissa scales.*

Synchronized average FIA/MS/MS ion chronograms of hexazinone in a reference standard and strawberry sample, and the resulting A_m vs. S_{norm} function

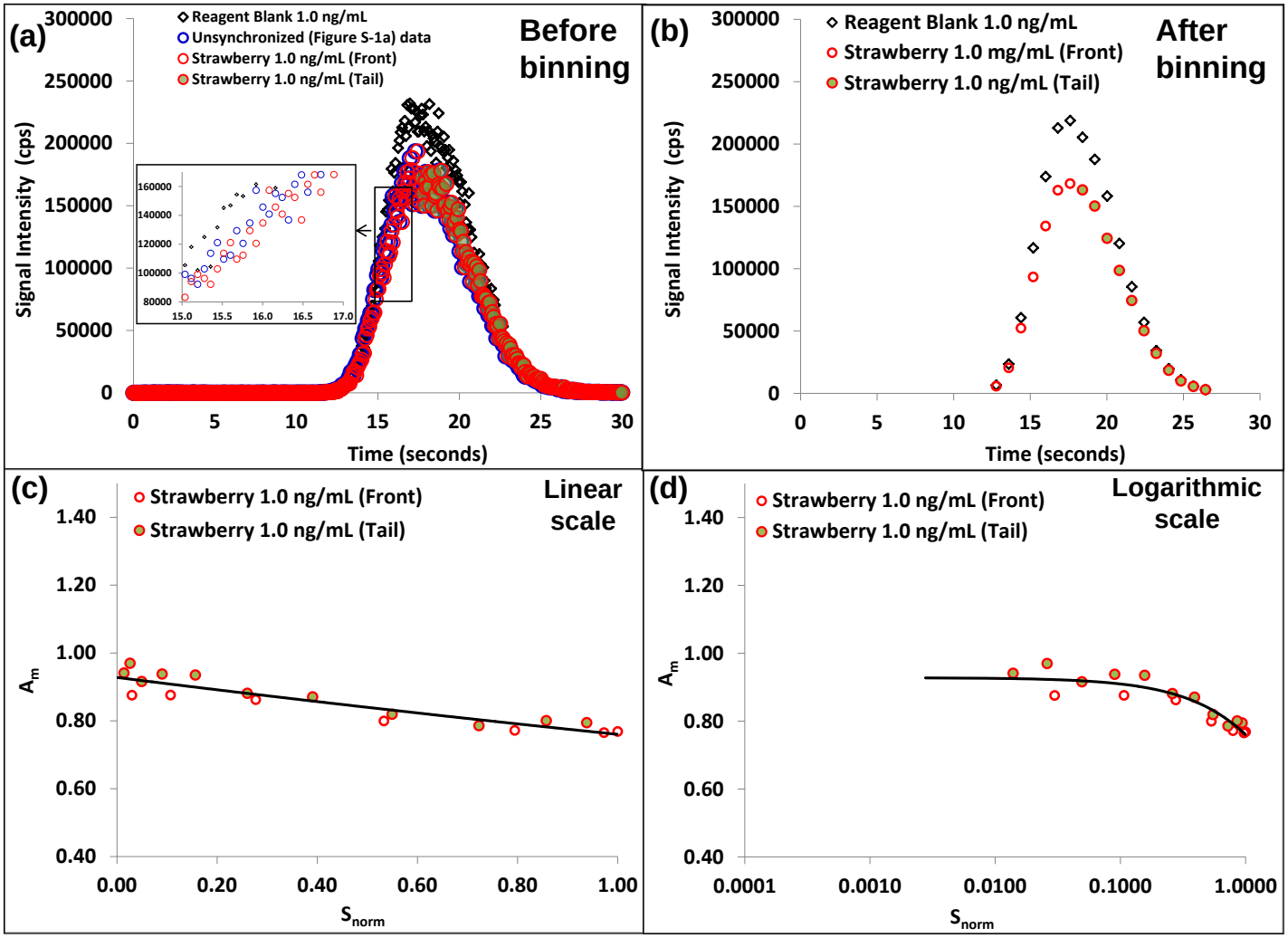

Figure S-2. *Calculation of A_m as a function of S_{norm} for hexazinone in strawberry extract from* ***synchronized*** *data. Averaged MS/MS chronograms: (a) all data points and (b) binned. The strawberry data shown on panel (a) has been shifted by +120 milliseconds (see inset). The resulting A_m vs. S_{norm} graphs are shown in (c) linear and (d) logarithmic abscissa scales.*

2.0 Supporting Data and Information

2.1 Experimental proof-of-concept: analysis of 3 pesticides in 5 matrices

Table S-3: *Trace-level quantitative analysis results obtained by the proposed method with first order exponential regression, equation 11,* $A_m(S_{norm}) = a \cdot e^{b(S_{norm})}$*, for samples of complex matrices that were spiked with the herbicides hexazinone, triflusulfuron methyl and flupyrsulfuron methyl.*

Matrix	Spike Level, ng/mL	Analyte								
		Hexazinone			**Triflusulfuron methyl**			**Flupyrsulfuron methyl**		
		a,b	A_0	% Acc.	a,b	A_0	% Acc.	a,b	A_0	% Acc.
Strawberry	1.00	0.929370, -0.202245	0.929	93	0.904353, 0.081249	0.904	90	0.888453, 0.120212	0.888	89
	5.00	4.39678, -0.19031	4.397	88	4.38821, 0.04045	4.388	88	4.45160, 0.02200	4.452	89
Wheat Grain	1.00	1.01538, -0.04038	1.015	102	0.987575, 0.123328	0.988	99	0.957949, 0.187538	0.958	96
	5.00	5.02024, -0.05831	5.020	100	5.19349, 0.04734	5.193	104	5.03991, 0.07730	5.040	101
Corn Meal	1.00	0.948488, -0.147927	0.948	95	0.983526, -0.172289	0.984	98	0.959487, -0.123701	0.959	96
	5.00	4.70071, -0.17310	4.700	94	5.36851, -0.23908	5.369	107	5.28373, -0.21202	5.284	106
Rat Urine	1.00	0.857536, -0.900458	0.858	86	0.882453, -0.329527	0.883	88	0.890162, -0.316513	0.890	89
	5.00	4.26758, -0.89614	4.268	85	3.78566, -0.21404	3.786	76	4.06447, -0.35474	4.064	81
Canola Seed	1.00	0.95614, -4.81960	0.956	96	n.d.	n.d.	n.d.	n.d.	n.d.	n.d.
	5.00	5.80433, -6.18468	5.804	116	n.d.	n.d.	n.d.	n.d.	n.d.	n.d.
Average %Accuracy		**Hexazinone 96 ± 9**			**Triflusulfuron methyl 94 ± 10**			**Flupyrsulfuron methyl 93 ± 8**		
Overall Average %Accuracy		**All analytes, all matrices 94 ± 9**								

Acc. = % Accuracy = 100(A_0/A).*

Table S-4: *Trace-level analysis results obtained by the proposed method with second order exponential regression, equation 12,* $A_m(S_{norm}) = a \cdot e^{b(S_{norm})} + c \cdot e^{d(S_{norm})}$, *for control samples that were spiked with the herbicides hexazinone, triflusulfuron methyl and flupyrsulfuron methyl.*

Matrix	Spike Level, ng/mL	Analyte								
		Hexazinone			Triflusulfuron methyl			Flupyrsulfuron methyl		
		a,b,c,d	A_0	% Acc.	a,b,c,d	A_0	% Acc.	a,b,c,d	A_0	% Acc.
Strawberry	1.00	0.93510, -0.26950, 0.00189, 3.48627	0.937	94	-5.89559, -0.88037, 6.80380, -0.72788	0.908	91	0.05776, 1.56998, 0.86875, -0.15663	0.927	93
	5.00	7.59473, -0.13864, -3.19780, -0.07171	4.397	88	4.6549, -0.0394, -0.6418, -12.4941	4.013	80	4.20715, -0.09252, 0.24015, 0.19244	4.447	89
Wheat Grain	1.00	-0.26742, 0.24990, 1.28179, 0.03773	1.014	101	0.87503, 0.28111, 0.22499, -8.37147	1.100	110	0.85794, 0.32057, 0.16291, -5.21982	1.021	102
	5.00	-13.8924, 0.8082, 18.8223, 0.7097	4.930	99	5.19341, 0.04791, 0.00038, -7.41488	5.194	104	13.7980, 0.3461, -8.7576, 0.4707	5.040	101
Corn Meal	1.00	2.03322, -0.09406, -1.08470, -0.04894	0.949	95	0.898646, -0.170663, 0.087153, -0.227450	0.986	99	0.17423, -5.06930, 0.84311, 0.03524	1.017	102
	5.00	6.33572, -0.14807, -1.63555, -0.08209	4.700	94	1.31637, -2.15604, 4.19431, 0.00399	5.511	110	1.46985, -1.88303, 3.94552, 0.05311	5.415	108
Rat Urine	1.00	0.87278, -1.05085, 0.00096, 4.41466	0.874	87	-0.27097, 0.01185, 1.15318, -0.22269	0.882	88	0.90089, -0.37483, 0.00004, 7.26472	0.901	90
	5.00	3.67362, -1.45694, 0.71079, 0.35182	4.384	88	4.61269, -0.18290, -0.82819, -0.06101	3.785	76	4.13322, -0.44737, 0.00189, 5.21115	4.135	83
Canola Seed	1.00	-1.41638, -3.79309, 2.37185, -4.12667	0.9555	96	n.d.	n.d.	n.d.	n.d.	n.d.	n.d.
	5.00	4.67972, -7.79346, 1.27632, -3.29742	5.956	119	n.d.	n.d.	n.d.	n.d.	n.d.	n.d.
Average %Accuracy		**Hexazinone 96 ± 9**			**Triflusulfuron methyl 95 ± 13**			**Flupyrsulfuron methyl 96 ± 8**		
Overall Average %Accuracy		**All analytes, all matrices 96 ± 10**								

Acc. = % Accuracy = 100(A_0/A).*

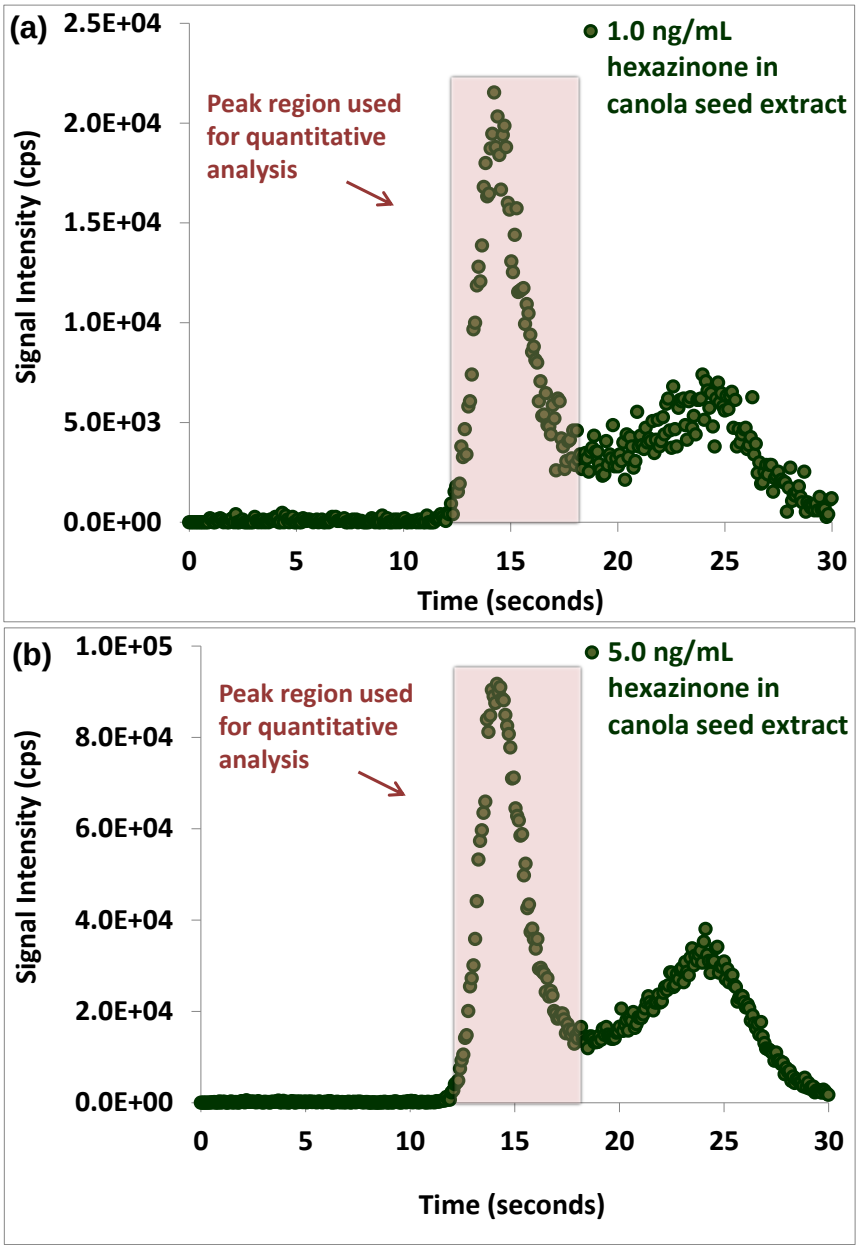

Figure S-3. *Expanded from Figure 4 (main article): split signal created by matrix effects in the ion chronogram of hexazinone (m/z 253 → m/z 171) in canola seed extracts at (a) 1.0 ng/mL and (b) 5.0 ng/mL. This occurs when matrix suppression effects weaken with dilution at a rate greater than signal reduction due to decreasing analyte concentration. The asymmetrical signal distortion was preliminarily attributed to residual of matrix components (e.g. oils) in/on the ion source which could result in prolonged matrix effects over the later time region, or analyte/matrix separation during flow injection analysis. For this reason and to ensure measurement accuracy, only peak-front data points were used (without binning) for analyte quantitation in canola seed. Split signals and asymmetrical signal distortions observed in FIA/MS with real-time infinite dilution are currently under further investigation.*

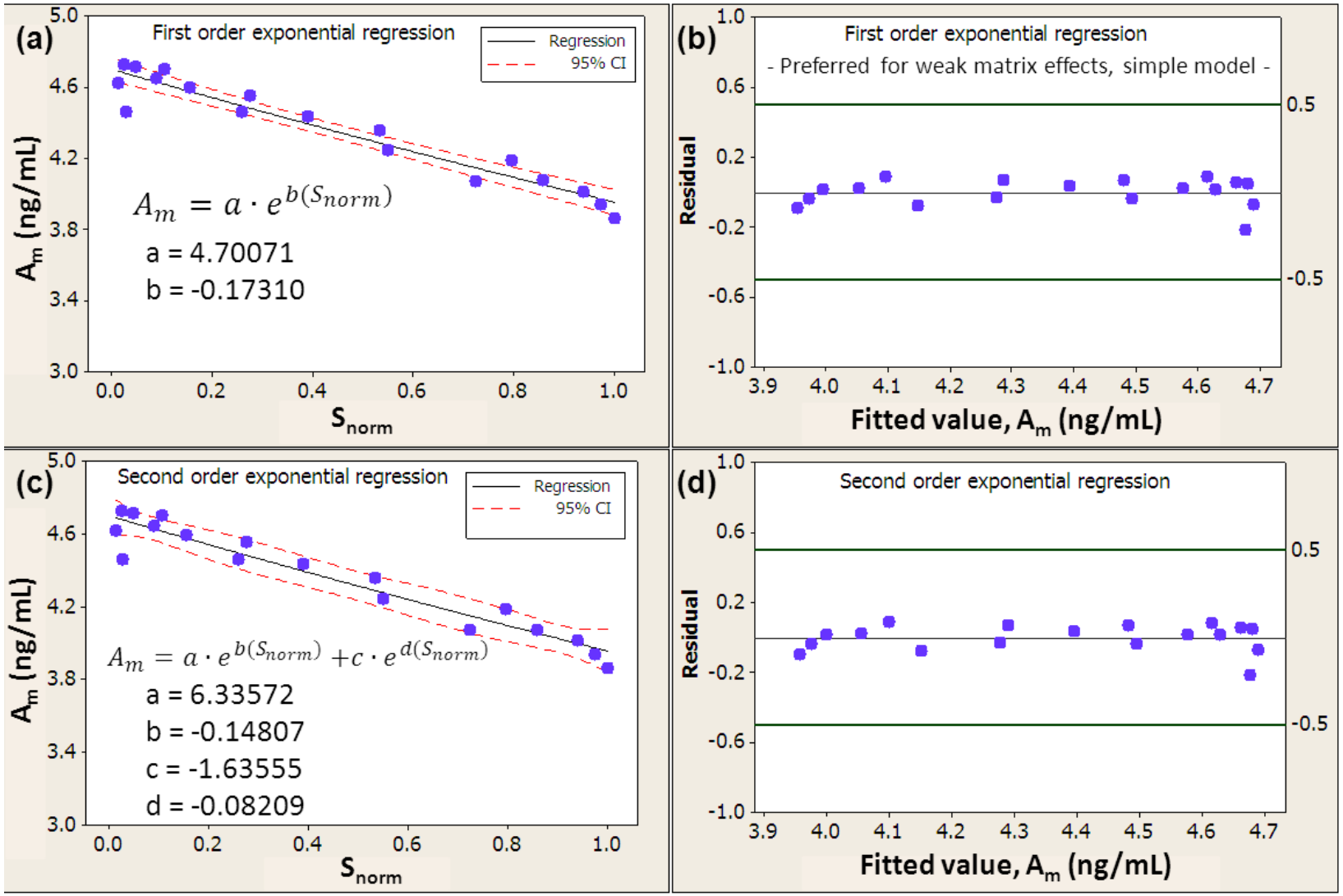

Figure S-4. *Non-linear regression results obtained for hexazinone in corn meal extract at 5.0 ng/mL. Top panels: (a) first order exponential regression and (b) corresponding residuals. Bottom panels: (c) second order exponential regression and (d) corresponding residuals. The residual plots have been scaled to the acceptable range, ± 20% of A, with reference lines at ± 10% of A.*

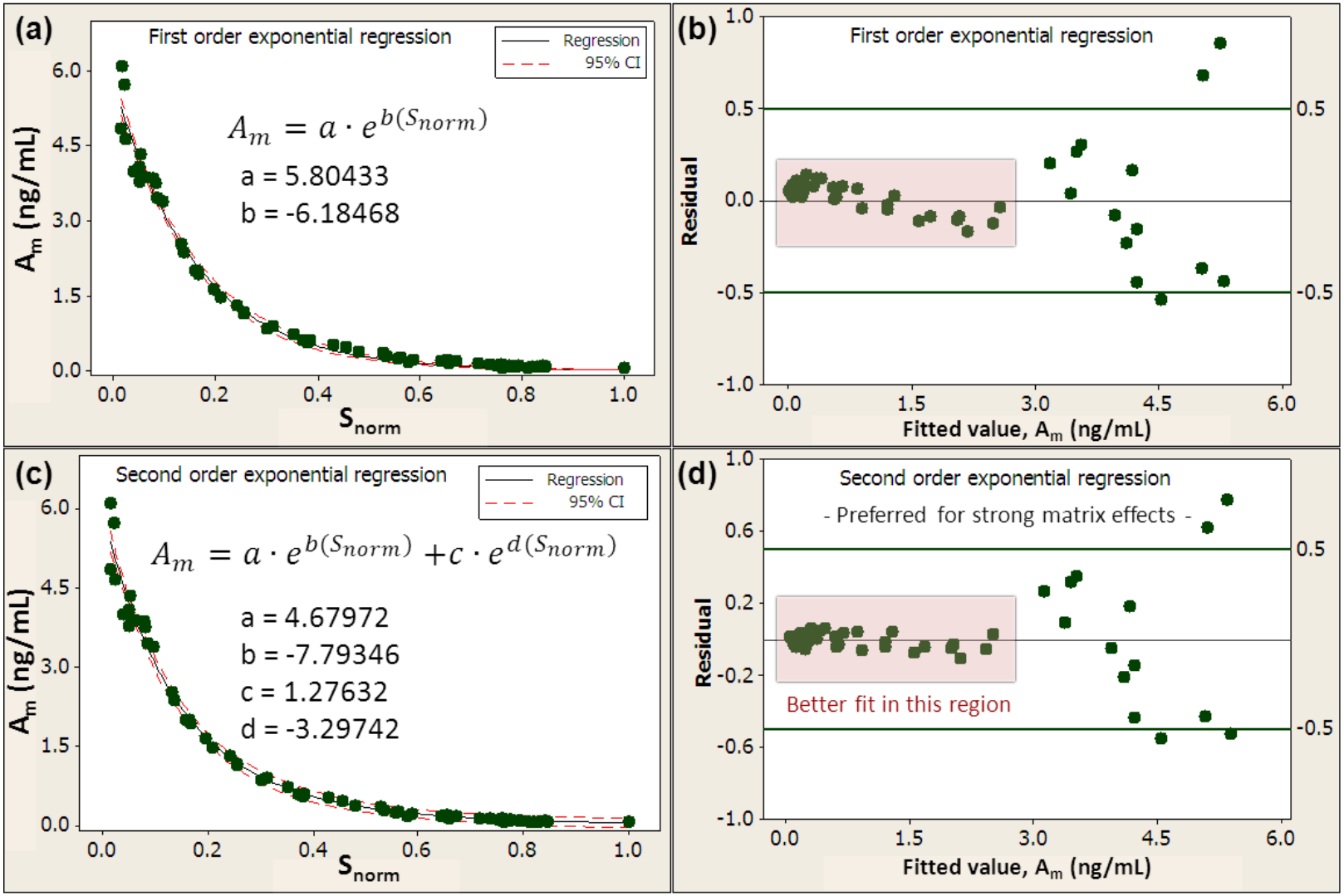

Figure S-5. *Non-linear regression results obtained for hexazinone in canola seed at 5.0 ng/mL. Top panels: (a) first order exponential regression and (b) corresponding residuals. Bottom panels: (c) second order exponential regression and (d) corresponding residuals. The residual plots have been scaled to the acceptable range, ± 20% of A, with reference lines at ± 10% of A.*

As exemplified in Figure S-4, the first order exponential regression performed consistently well in the presence of minor matrix effects; therefore, it is recommended for those cases as a simple yet reliable model. On the other hand, the second order exponential model was occasionally unstable when matrix effects were minor. However, when strong matrix effects were encountered, the second order exponential regression performed very well and better than the first order model. An even greater difference between the performance of the first and second order exponential models in the presence of strong matrix effects was observed in other cases, such as chlorantraniliprole in strawberries, shown in Figure 6 (main manuscript). Consequently, the second order exponential regression is recommended as the most reliable model out of the two tested for cases with strong matrix effects. Also noticeable in residual plots is an increase in measurement uncertainty that occurs as the signal-to-noise ratio decreases with sample dilution. This effect was observed in several cases, including data displayed in Figures S-5 and 6.

2.2 Quantitation of chlorantraniliprole in strawberry field samples

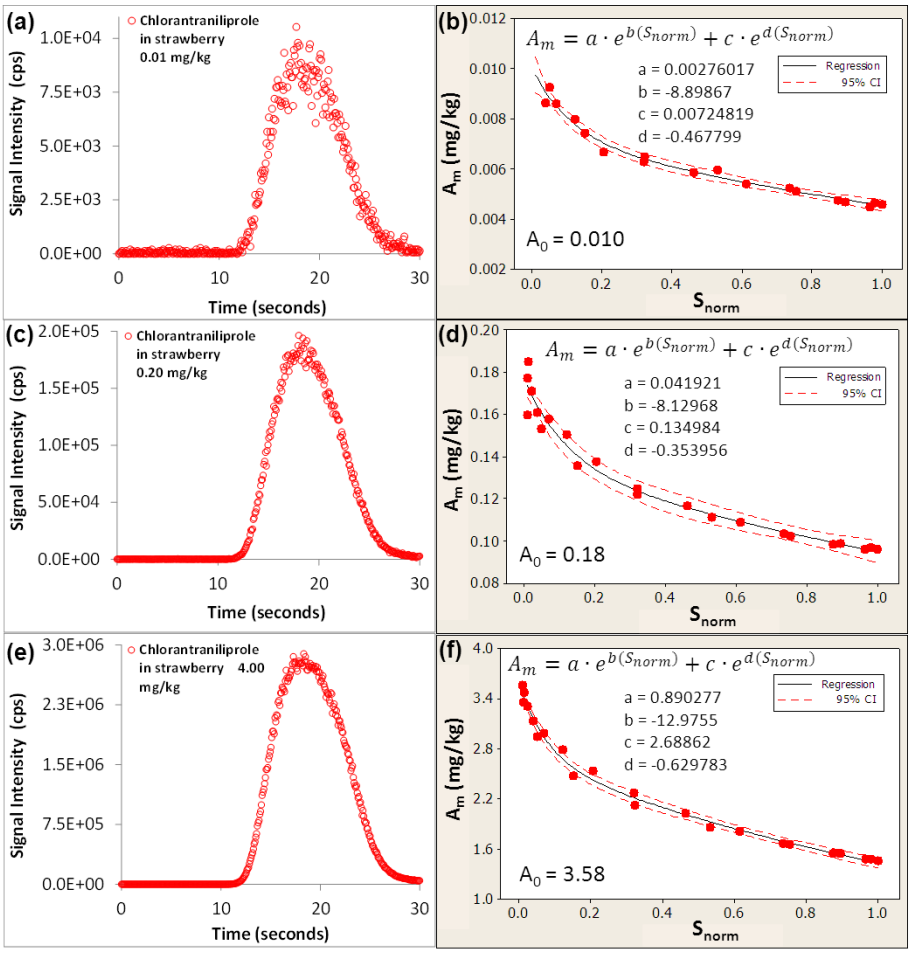

Figure S-6. *Raw MS/MS ion chronograms (m/z 484 → m/z 453) obtained for the analysis of control strawberry samples that were fortified with chlorantraniliprole at (a) 0.01 mg/kg, (c) 0.20 mg/kg and (e) 4.00 mg/kg with their corresponding A_m vs. S_{norm} graphs and second order exponential regression results shown in panels (b), (d), and (f), respectively. This experiment demonstrated that accurate results can be obtained with the proposed method across low, medium and high analyte concentrations.*

2.3 Quantitative analysis with detector saturation conditions

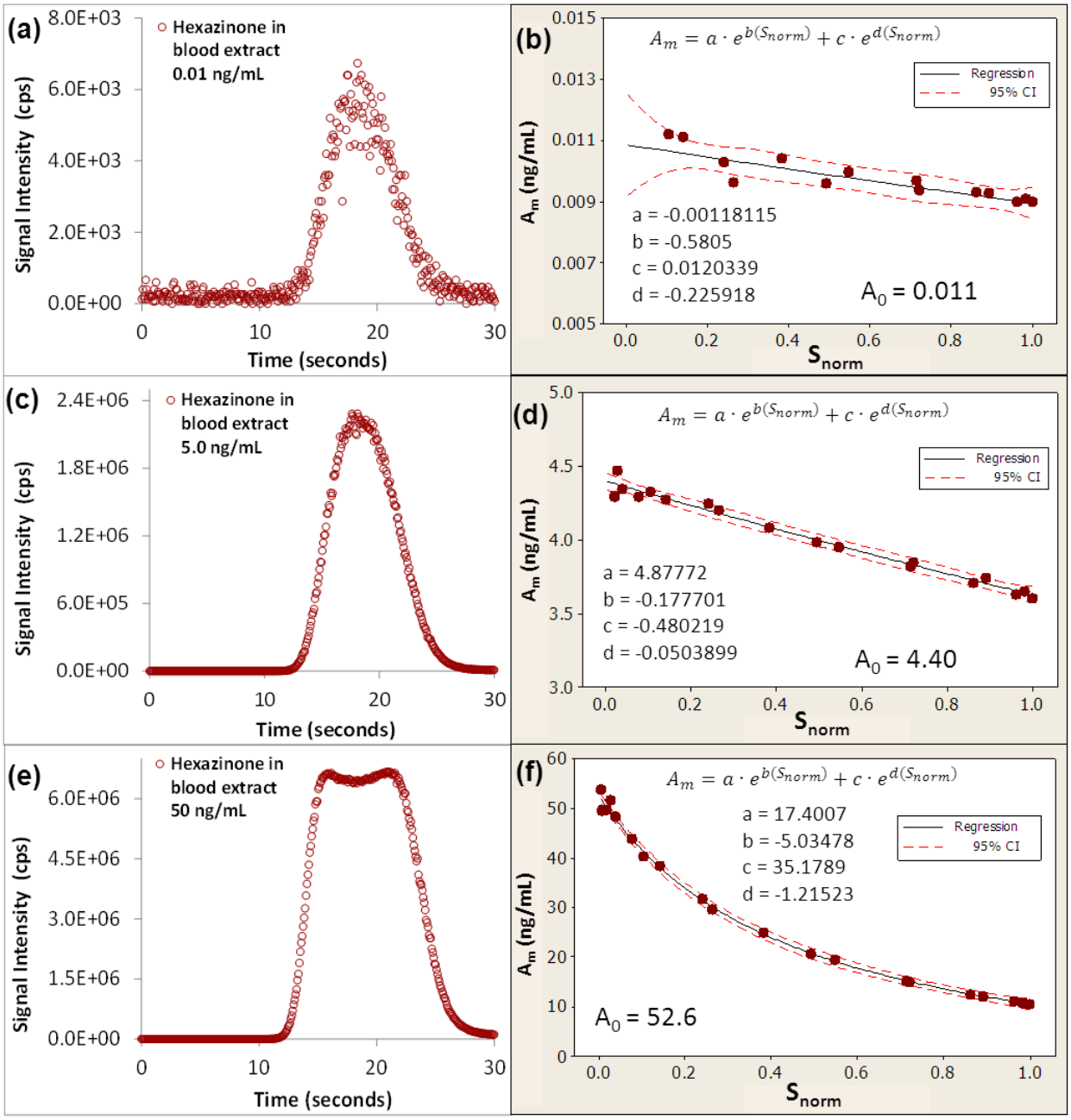

Figure S-7. *Representative raw ion chronograms obtained for hexazinone in blood extract matrix. Left panels (a) 0.01 ng/mL, (c) 5.0 ng/mL and (e) 50 ng/mL with their corresponding A_m vs. S_{norm} graphs and second order regression results shown on the right panels (b), (d), and (f), respectively. Note that detector saturation is evident in panel e, yet an accurate result was obtained. Overall, the method applicable concentration range for quantitation of hexazinone in rat blood extracts is 0.01 ng/mL to 100 ng/mL. This range is equivalent to 1.0 ng/mL to 10,000 ng/mL in blood samples, based on the sample preparation procedure used (see experimental section in the main manuscript).*

2.4 Derivation of ME(S_{norm}) functions shown in equations 15, 16, and 17

Matrix effects can be defined as a function of time in flow injection analysis. Therefore, from equation 3 we obtain that

$$\mathrm{ME(t)} = \frac{\mathrm{R_{AM}(t)}}{\mathrm{R_A(t)}} = \frac{\mathrm{I_{AM}(t)/A}}{\mathrm{I_A(t)/A}} = \frac{\mathrm{I_{AM}(t)}}{\mathrm{I_A(t)}} \qquad \text{(equation S-1)}$$

Where $I_A(t)$ and $I_{AM}(t)$ are the time-dependent signal intensity functions for an analyte in a clean standard solution and a sample that contains matrix, respectively.Now, equation S-1 can be expressed as a function of normalized sample concentration (S_{norm}) because the time dependency of signal intensity in flow injection analysis arises from the varying sample concentration, yielding the following expression:

$$\mathrm{ME(S_{norm})} = \frac{\mathrm{I_{AM}(S_{norm})}}{\mathrm{I_A(S_{norm})}} \qquad \text{(equation S-2)}$$

Based on equation 9 from the main article, $A_m(t)$ can be re-written as follows:

$$\mathrm{A_m(t)} = \frac{\mathrm{I_{AM}(t)}}{\mathrm{R_A(t)}} = \frac{\mathrm{I_{AM}(t)}}{\mathrm{I_A(t)/A}} = \mathrm{A} \cdot \frac{\mathrm{I_{AM}(t)}}{\mathrm{I_A(t)}} \qquad \text{(equation S-3)}$$

Note that, in principle and for mathematical purposes, A (analyte concentration in the injected solution) is equal to A_0. Therefore, A_0 can replace A in equation S-3. Also, expressing equation S-3 as a function of S_{norm} results in the following expression:

$$\mathrm{A_m(S_{norm})} = \mathrm{A_0} \cdot \frac{\mathrm{I_{AM}(S_{norm})}}{\mathrm{I_A(S_{norm})}} \qquad \text{(equation S-4)}$$

Therefore, merging equations S-2 and S-4 results in equation 15 in the main article: $\mathrm{ME(S_{norm})} = \frac{\mathrm{A_m(S_{norm})}}{\mathrm{A_0}}$. Considering that $\lim_{\mathrm{S_{norm}} \to 0+} \mathrm{A_m(S_{norm})} = \mathrm{A_0}$ (main article, equation 10) and merging equations 11 and 12 with equation 15 results in:

$$\mathrm{ME(S_{norm})} = \mathrm{e^{b \cdot (S_{norm})}} \qquad \text{(main article, equation 16)}$$

$$\mathrm{ME(S_{norm})} = \frac{\mathrm{a \cdot e^{b(S_{norm})} + c \cdot e^{d(S_{norm})}}}{\mathrm{a+c}} \qquad \text{(main article, equation 17)}$$